

Characterization of the mechanical properties of cross-linked serum albumin microcapsules: effect of size and protein concentration

Jonathan Gubspun¹ · Pierre-Yves Gires² · Clément de Loubens¹ ·
Dominique Barthès-Biesel² · Julien Deschamps¹ · Marc Georgelin¹ · Marc Leonetti¹ ·
Eric Leclerc² · Florence Edwards-Lévy³ · Anne-Virginie Salsac²

Received: 28 July 2015 / Revised: 22 March 2016 / Accepted: 24 April 2016 / Published online: 10 June 2016
© Springer-Verlag Berlin Heidelberg 2016

Abstract A microfluidic technique is used to characterize the mechanical behavior of capsules that are produced in a two-step process: first, an emulsification step to form droplets, followed by a cross-linking step to encapsulate the droplets within a thin membrane composed of cross-linked proteins. The objective is to study the influence of the capsule size and protein concentration on the membrane mechanical properties. The microcapsules are fabricated by cross-linking of human serum albumin (HSA) with concentrations from 15 to 35 % (*w/v*). A wide range of capsule radii (~40–450 μm) is obtained by varying the stirring speed in the emulsification step. For each stirring speed, a low threshold value in protein concentration is found, below which no coherent capsules could be produced. The smaller the stirring speed, the lower the concentration can be. Increasing the concentration from the threshold value

and considering capsules of a given size, we show that the surface shear modulus of the membrane increases with the concentration following a sigmoidal curve. The increase in mechanical resistance reveals a higher degree of cross-linking in the membrane. Varying the stirring speed, we find that the surface shear modulus strongly increases with the capsule radius: its increase is two orders of magnitude larger than the increase in size for the capsules under consideration. It demonstrates that the cross-linking reaction is a function of the emulsion size distribution and that capsules produced in batch through emulsification processes inherently have a distribution in mechanical resistance.

Keywords Microcapsules · Interfacial cross-linking · Serum albumin · Microfluidics · Mechanical properties · Identification

P.Y. Gires and J. Gubspun contributed equally to this work

✉ Marc Leonetti
leonetti@irphe.univ-mrs.fr

✉ Anne-Virginie Salsac
a.salsac@utc.fr

¹ IRPHE (UMR CNRS 7342), Aix Marseille Université - Cnrs - Centrale Marseille, Marseille, France

² Laboratoire de Biomécanique et de Bioingénierie BMBI (UMR CNRS 7338), Université de technologie de Compiègne, Sorbonne université - CNRS, Compiègne, France

³ Institut de Chimie Moléculaire de Reims ICMR (UMR CNRS 7312), Université de Reims Champagne-Ardenne, Reims, France

Introduction

Capsules consist of droplets enclosed by a membrane with shear resistant properties. Among all their industrial and clinical applications, one can highlight their extensive use in cosmetics and the great potential they offer in bioengineering and in medicine: by encapsulating drugs, genetic material, or cells, capsules have found applications in targeted drug delivery [2, 15, 16, 21] and in the development of bioartificial organs and biosensors [12, 23, 27]. In most applications, the release and protection of the internal medium need to be strictly controlled.

Capsules can be produced in batch. A classical technique consists of first producing an emulsion and then a membrane around the droplets through a reaction of interfacial

cross-linking. Here, we focus on capsules with a human serum albumin (HSA) membrane cross-linked with an acyl dichloride. These capsules are well adapted for drug delivery systems and more appropriate for biomedical applications [10] than ovalbumin ones. Ovalbumin is, indeed, typically less pure than HSA, as it often contains a small amount of other constituents such as lipids.

Albumin microcapsules have been extensively studied over the last two decades, both in terms of fabrication process and resulting properties. The cross-linking degree of HSA microcapsules has mainly been determined through Fourier transform infrared spectroscopy [22] and TNBS assay [1], which enabled to assess the effect of some of the preparation parameters: the reaction pH, reaction time, and cross-linker concentration have been shown to influence the extent of the reaction between acyl dichloride and acylable groups (hydroxyl, amine, and carboxylate residues) of the protein. The link between cross-linking degree of the capsule membranes and their mechanical properties has then been investigated by Chu et al. [5]. Other parameters of the preparation procedure have, however, not yet been explored. Among them are the protein concentration in the initial aqueous phase and the stirring speed chosen for the emulsification step, which both govern the total available protein at the interface of the emulsion. These parameters are very likely to have an impact on the cross-linking degree of the capsule membranes, and therefore to influence their mechanical properties.

It is usually assumed that capsules prepared under given physico-chemical conditions are identical and have the same physical properties. But, to our knowledge, no study has ever investigated whether this is the case, when both the stirring speed (and thus the capsule size) and the protein concentration are varied on a wide range. Understanding the link between physico-chemical conditions and mechanical properties is, however, an essential step for a proper control of the fabrication process and of the protection/release of the encapsulated inner content. But characterizing the mechanical behavior of microcapsules is challenging owing to their sub-millimetric size.

Various techniques exist to estimate the mechanical properties of the capsule membrane. One approach consists in applying a local stress on a single capsule, either through micropipette aspiration [13], compression between two parallel plates [4], or compression with an atomic force microscope (AFM) [9, 25]. Each technique is by essence designed for a limited range of capsule size and mechanical resistance. For instance, the compression method is adequate for millimetric capsules and can be applied to soft or hard capsules [24]. The micropipette aspiration has, however, only been applied on soft micro-particles such as cells, vesicles, and polymersomes [8], the size of which is of the order of a few micrometers at most. None of these techniques is

hence designed to characterize the mechanics of capsules with radii ranging from a few tens to a few hundreds of micrometers.

A powerful technique to measure capsule mechanics is to observe the deformation of capsules under flow. The mechanical properties of the capsule membrane are obtained by comparing the experimental deformed shapes to the ones predicted by a mechanical model of the system [5, 18]. Compared to techniques applying local stress, hydrodynamical techniques exert distributed forces on the entire membrane. They also allow to measure capsule populations in batch, as it is possible to convect the particles automatically toward the observation area.

Different hydrodynamic methods have been used to characterize capsules with radii within the challenging range. One of them consists of flowing the capsules in a transparent microcapillary tube with transverse dimensions comparable to the capsule one. It has been applied to characterize the mechanical properties of microcapsules (radius ranging from 30 to 60 μm) with a cross-linked ovalbumin membrane using circular [5, 18] and square-section [14] channels. Specifically, it has been shown that the shear elastic modulus of the membrane depends on the pH and reaction time of the cross-linking reaction [5].

Another hydrodynamic technique consists of deforming capsules in a known planar elongation flow using a microfluidic cross-flow chamber [19, 20]. As the capsule is far from the channel walls of the chip, the shear elastic modulus can be determined on a large range of sizes from 50 to 200 μm within the same chamber. The method is currently limited to soft particles. A first study has been conducted on capsules with a HSA membrane, subjected to weak deformations (linear regime) [19]. It is found that the shear elastic modulus increases with the HSA concentration, as expected, but also with the size of capsules. This unexpected result was later confirmed in the regime of large deformation (nonlinear regime) [20]. However, the two studies do not overlap in size and albumin concentrations: there is thus the need for a systematic study of the effect of size and polymer concentration on the mechanical properties of HSA capsules.

The present objective is to systematically characterize the mechanical properties of HSA capsules under moderate deformation by a careful study of the variation of mechanical resistance with capsule radius and initial protein concentration. The pore flow technique will be used on a notably larger range of capsule sizes compared to previous studies, the capsules being produced under various emulsification stirring speeds. The HSA concentration will also be varied to see its influence on the mechanical properties. After having detailed the fabrication method, we will overview in “[Material and methods](#)” section how the capsules were characterized. The influence of the capsule size

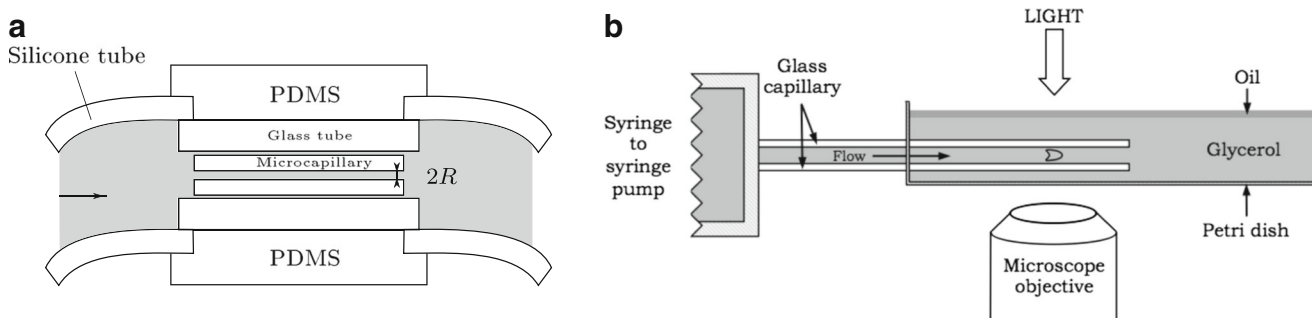


Fig. 1 **a** Setup 1, designed for small-size microcapsules ($a \leq 80 \mu\text{m}$): $R \in \{50, 75\} \mu\text{m}$. **b** Setup 2, designed for larger size microcapsules ($a \geq 130 \mu\text{m}$): $R \in \{150, 200, 300, 400\} \mu\text{m}$

and protein concentration will be shown in “**Results**” section and discussed in “**Discussion**” section in order to provide a possible explanation of the correlation between the measured mechanical properties and the physico-chemistry of the cross-linking reaction.

Material and methods

Experimental procedure

The experimental procedure is similar to the one described in Lefebvre et al. [18]. The capsules are prepared from an emulsion of droplets of aqueous-buffered HSA solutions (pH 8) suspended in cyclohexane added with a surfactant (sorbitan trioleate). The cross-linking reaction is started by adding to the emulsion a saturated solution of terephthaloyl chloride in a solvent composed of chloroform and cyclohexane (1:4 V:V). During this step, the two activated groups of the cross-linker react with the available acylable groups of HSA at the interface of each aqueous droplet, forming amide, ester, and anhydride bonds from amine, hydroxyl, and carboxylic acid residues of HSA, respectively. The reaction time is 30 min. Various mass concentrations of HSA are considered: $[\text{HSA}] = 15\text{--}35 \%$ (w/v), which correspond to 15–35 g of solute dissolved in 100 ml of pH 8 aqueous buffer. In the following, the different capsule batches will be denoted HSA n , where n corresponds to the HSA concentration. Three stirring speeds are used for the formation of the emulsion: 625, 1000, and 1700 rpm.

After fabrication, the capsules are rinsed successively in an aqueous solution containing polysorbate as surfactant, and finally thrice in pure water. The average diameter of the resulting capsules has been determined by laser diffraction (Malvern Mastersizer 2000). A strong influence of the capsule size with the stirring speed has been observed. For instance, the diameter values measured for the HSA20 capsules after rinsing are 418 μm (span 1.16) at 625 rpm, 204 μm (span 0.95) at 1000 rpm, and 57 μm (span 0.65)

at 1700 rpm. The HSA concentration, however, modulates very slightly the capsule size. The capsules are then transferred into glycerol for storage. The glycerol rapidly diffuses inside the capsule, so that the internal and external contents are identical and consist of glycerol with negligible water content.

A dilute suspension of capsules is prepared by re-suspending a volume of the stored capsules in pure glycerol (e.g. 40 μL in 2 ml). A syringe pump is used to flow the suspension through a glass microchannel (Hampton Research, Vitrocom and Beckman Coulter) with internal radius R of the same order as the capsule radius (50, 75, 150, 200, 300, and 400 μm). The temperature of the experiment is monitored in order to get a precise value of the glycerol viscosity. Videos of the capsules are recorded with a high-speed camera mounted on a microscope.

Owing to the large variation in capsule size when the stirring speed is changed, the experiments had to be performed with two different setups (Fig. 1). Setup 1, which is dedicated to small capsules ($a \leq 80 \mu\text{m}$), is of the same type as the one described in Chu et al. [5]. Setup 2 is a new experimental setup designed for larger capsules ($a \geq 130 \mu\text{m}$). It is directly connected to the syringe pump on the one side and immersed into a reservoir filled with glycerol on the other, in order to re-suspend the capsules. It is covered by a layer of oil to avoid water dissolution into it, as water has a strong effect on the viscosity of glycerol [11]. It enables to flow one capsule back and forth under varying flow rates for a given capsule, which was not possible with the setup designed for small capsules.

Prior to conducting experiments, the dependency of the viscosity of the external fluid on temperature has been determined using rheometers in cone-plane geometries (setup 1: Thermo Haake 1, diameter 60 mm, angle 2° ; setup 2: Thermo Haake Mars 3, diameter 60 mm, angle 2°). The viscosity is thus deduced from the measurement of the solution temperature during the experiment. Despite the large influence that temperature has on the glycerol viscosity, we have managed to reach a good accuracy: the average error

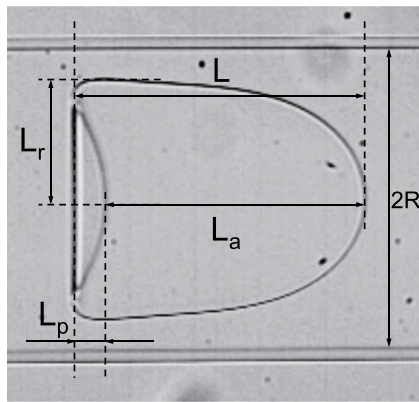


Fig. 2 Typical deformed profile of a capsule. Definition of the geometrical parameters L , L_r , L_p , and L_a

on viscosity is calculated to be about 7 % for setup 1 and 2 % for setup 2, taking into account both the rheometer and temperature uncertainties.

Capsule profile analysis

As can be seen in Fig. 2, the initially spherical capsules can be significantly deformed as they flow in the channel. The velocity V of each capsule is deduced from the distance traveled by the front of the capsule while it crosses the microscope observation window. The capsule deformed profile and the microchannel radius R are also extracted from the images. The capsule initial radius a is deduced from the volume computed by rotating a half profile around the axis. The radius value, thus obtained, has been verified in setup 2 where capsules can also be observed at zero velocity for $a < R$.

The deformation of the initially spherical capsules is quantified by the total length L , the axial length L_a , the radial length L_r , and the cross-section surface area S (Fig. 2). We also define the parachute depth $L_p = L - L_a$. As the profile can be slightly asymmetric, L , L_r , L_p , and a are the average values obtained from the upper and lower half profiles. The capsules are discarded from further analysis if their recorded shape is too far from axisymmetric. For instance, capsules are discarded if the relative difference between the upper and lower half-profiles is larger than 6 % for L , 4 % for S , and 2 % for a .

The determination of the capsule deformed profile is inherently associated with experimental errors. Table 1 summarizes the values of the maximum uncertainty that are tolerated on the various quantities determined from the images of the capsule profiles.

Model

The mechanical model of a capsule flowing under constant flow rate in a cylindrical tube of comparable size is solved numerically [7, 17]. The flow field and the capsule profile are fully axisymmetric. The model assumptions are only briefly outlined; more details may be found in the above cited references.

The capsules are assumed to be spherical at rest and to have a membrane made of an infinitely thin strain-softening neo-Hookean material. This constitutive law is adapted for the moderate capsule deformations that are presently considered. For the neo-Hookean law, the principal Cauchy in-plane tensions (forces per unit arc length of deformed surface curves) can be expressed as [3]

$$\tau_1 = \frac{G_s}{\lambda_1 \lambda_2} \left[\lambda_1^2 - \frac{1}{(\lambda_1 \lambda_2)^2} \right] \quad (\text{likewise for } \tau_2), \quad (1)$$

in which the in-plane deformation is measured by the principal extension ratios λ_1 and λ_2 . The mechanical resistance of the membrane is provided by the surface shear modulus G_s . The microcapsules are assumed to be neutrally buoyant and inertialess owing to their small size. As the internal and external liquids are incompressible and Newtonian (viscosity μ), both flow fields satisfy the Stokes equations.

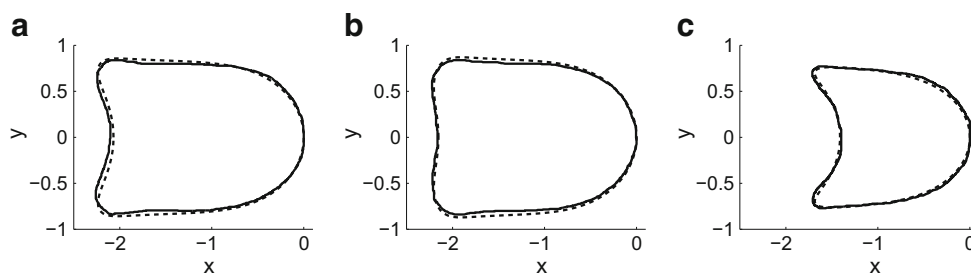
At steady state, if any, the capsule velocity and deformed shape only depend on the size ratio a/R and capillary number $Ca = \mu U/G_s$, where U is the mean unperturbed velocity of the external liquid. The size ratio is a measure of confinement, while the capillary number measures the ratio between the characteristic viscous and elastic forces.

The model yields the deformed profile of the capsule as a function of a/R and Ca . A database was created tabulating the capsule geometric characteristics L/a , L_a/a , L_r/a , S/a^2 , and velocity ratio V/U as a function of a/R and Ca [5]. A piecewise linear interpolation is performed in the $(a/R, Ca)$ space in order to have data points every 0.001 in Ca and 0.005 in a/R . Owing to the strain-softening

Table 1 Uncertainties over the measured values on the capsules

Measured quantity	L (μm)	L_a (μm)	L_p (μm)	L_r (μm)	a (μm)	$\Delta S/S$ (%)	R (μm)
Uncertainty	6	6	6	3	1	4	1

Fig. 3 Comparison between measured (solid line) and numerical profiles (dashed line). **a** HSA20: $a = 75 \mu\text{m}$, $a/R_{\text{sim}} = 0.98$, $Ca_{\text{sim}} = 0.05$; **b** HSA25: $a = 75 \mu\text{m}$, $a/R_{\text{sim}} = 0.99$, $Ca_{\text{sim}} = 0.04$; **c** HSA30: $a = 62 \mu\text{m}$, $a/R_{\text{sim}} = 0.79$, $Ca_{\text{sim}} = 0.11$



behavior of the neo-Hookean law, there exists a maximum capillary number Ca_{max} above which no steady state exists [5]. The values of Ca_{max} as a function of the size ratio a/R were interpolated and incorporated in the uniformly distributed database. In this way, we were able to check that the capillary number Ca used in experiments was sufficiently smaller than Ca_{max} to ensure the validity of our method (regime of moderate deformations).

Inverse analysis method

We have developed an algorithm to automatically perform the inverse analysis of capsule profiles. We only consider capsules with a size ratio $a/R \in [0.7, 1.2]$, which has been shown to be the optimal size ratio range for the inverse analysis [18].

For each analyzed capsule, we determine the ensemble of size ratios and capillary numbers $\{a/R, Ca\}$ for which the experimental and numerical values of geometrical parameters $\{a/R, L/R, L_a/R, L_p/R, L_r/R, S/R^2\}$ correspond to one another, within the tolerances indicated in Table 1. We then define independently the mean values of the capillary number \overline{Ca} and of the size ratio $\overline{a/R}$. The value \overline{Ca} is compared to the critical capillary number $Ca_{max}(a/R)$, above which no steady state exists. The capsule is excluded if $\overline{Ca} > Ca_{max} - 0.01$ in order to avoid potentially unsteady situations. Furthermore, if the capsule rear concavity is larger than the highest possible value in the database, the capsule is also excluded, as it may not have reached a steady state or be breaking up. For each couple of values $\{a/R, Ca\}$, the database provides the values of the velocity ratio V/U . The membrane shear modulus is then given by:

$$G_s = \frac{\mu V}{Ca(V/U)}, \quad (2)$$

where the capsule velocity V is measured experimentally. We obtain the ensemble of all possible shear moduli and calculate the mean and standard deviation, denoted $\overline{G_s}$ and σ , respectively.

The deformation of the capsule may be estimated by the mean elongation ratio Λ , which is defined as the deformed

profile perimeter divided by $2\pi a$. At low Ca , the deformation of the capsule is close to the experimental uncertainties (typically $\Lambda < 1.03$). We thus restrict our analysis to capsules for which the flow strength is large enough to induce significant capsule deformations ($\Lambda \geq 1.04$).

Results

Comparison between experimental and numerical shapes

Most capsules can be described by the numerical model, with a global success rate of 89 % (evaluated over more than 200 capsules). In particular, all the mechanical properties of all the small capsules (radius in the 40–80 μm range) can be identified.

Comparisons of experimental and numerical profiles are provided in Fig. 3. For each case, the values used in the numerical simulation are such that $Ca_{\text{sim}} = \overline{Ca}$ and $a/R_{\text{sim}} = \overline{a/R}$. As shown in Fig. 3, there is an excellent fit between the experimental and numerical profiles.

The values of surface shear modulus $\overline{G_s}$ are shown in Fig. 4 as a function of the mean elongation ratio Λ for

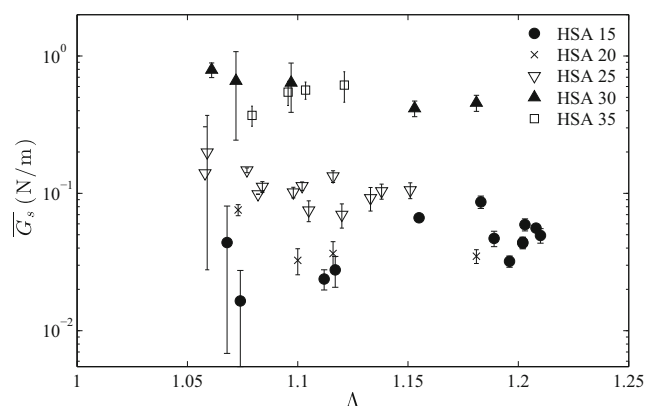


Fig. 4 Values of surface shear modulus $\overline{G_s}$ measured on capsules produced at 1700 rpm and of size $a = 65 \pm 5$. They are plotted as a function of the mean elongation ratio Λ for the different HSA concentrations. The error bars correspond to $\pm\sigma$

small capsules. In order to exclude any effect of the capsule size, the results indicated in the figure are for capsules of radius $a = 65 \pm 5 \mu\text{m}$. For a given HSA concentration, the data point are generally uniformly distributed about a mean value, even for fairly large membrane deformation ($\Lambda > 1.15$). The fact that the identification procedure predicts a constant value of surface shear modulus for all the values of deformation Λ indicates that the shear-softening model used in the inverse analysis is appropriate to describe the HSA membrane behavior within the level of the moderate deformation of the present experiments. Figure 4 also shows that the surface shear modulus increases with the HSA concentration, as further discussed in “Influence of the HSA concentration” section.

Influence of the HSA concentration

The HSA concentration effect is studied in detail for small capsules of radius in the range 40–80 μm , all produced with a 1700 rpm stirring speed. The HSA concentration is varied from 15 to 35 % (Fig. 5). No clear difference is found for the low concentrations (15 and 20 %), which was already apparent in Fig. 4. The surface shear modulus $\overline{G_s}$, however, increases significantly with the HSA concentration for $[\text{HSA}] \geq 20\%$. Figure 5 also indicates that, even in the 40–80 μm size range, $\overline{G_s}$ increases with capsule size for a given HSA concentration.

Averaged values $\langle \overline{G_s} \rangle$ of the surface shear moduli have been calculated for each concentration on capsules within a smaller size range (55–80 μm) in order to limit the influence of capsule size and isolate the effect of HSA concentration. As shown in Fig. 6, $\langle \overline{G_s} \rangle$ increases by about one order of magnitude when the [HSA] increases from 20 to 30 %. The average values of the surface shear modulus

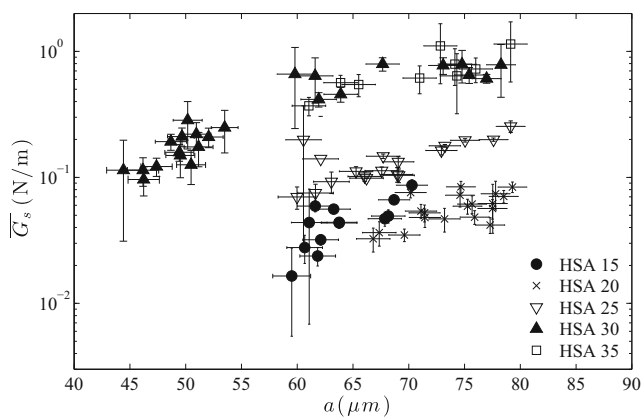


Fig. 5 Influence of HSA concentration on the surface shear modulus $\overline{G_s}$ for capsule sizes in the range $a \in [40, 80] \mu\text{m}$. The error bars correspond to $\pm\sigma$

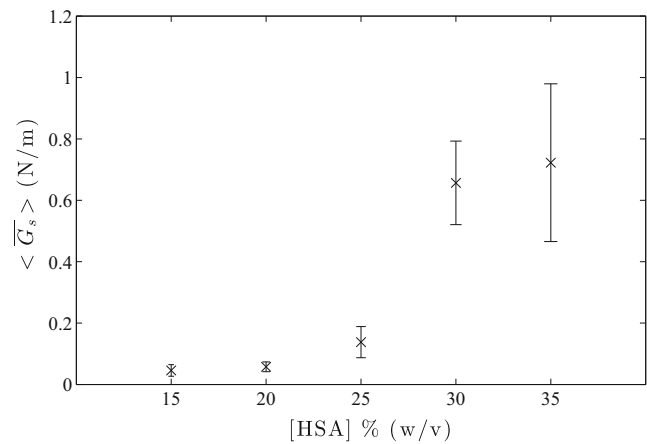


Fig. 6 Influence of the HSA concentration on the mean value of surface shear modulus $\langle \overline{G_s} \rangle$ calculated over the ensemble of capsules with $a \in [55, 80] \mu\text{m}$. The error bars correspond to the standard deviation σ over $\overline{G_s}$

are, however, almost identical for the concentrations of 15 to 20 %.

A statistical analysis of the values has been performed after transforming the values of $\overline{G_s}$ to obtain a normal distribution. They were subsequently analysed with the Statistical Analysis Toolbox of MATLAB R2013a using the one-way analysis of variance technique (“one-way ANOVA”) with the HSA concentration as factor. The averaged values $\langle \overline{G_s} \rangle$ calculated on a sample of 69 capsules were significantly higher when the HSA concentration increased from 15 to 30 % ($p < 0.001$). The variation was, however, not significant, when the concentration was further increased from 30 to 35 % ($p = 0.65$).

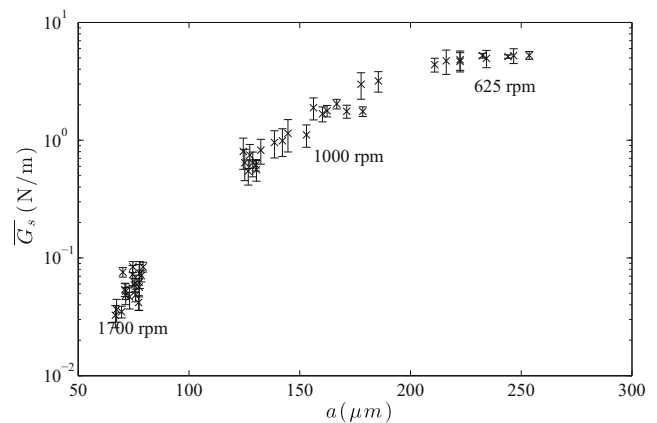


Fig. 7 Evolution of the surface shear modulus $\overline{G_s}$ as a function of the capsule radius a for the HSA20 capsules. The error bars correspond to $\pm\sigma$

Influence of size

The effect of size is studied on HSA20 capsules produced with the three stirring speeds. The tested capsules had a radius ranging from 65 to 260 μm . The evolution of the surface shear modulus $\overline{G_s}$ is shown in Fig. 7 as a function of the capsule radius. The trend toward an increase in surface shear modulus with size is not only visible over all the measurements, but it is also clearly present within each capsule population corresponding to a given stirring speed. A major unexpected result is the striking increase of G_s with size for a given HSA concentration: G_s increases sharply by more than two orders of magnitude, when the radius is only increased by a factor 5.

Discussion

The present study shows that capsules made of cross-linked HSA molecules can be characterized mechanically by flowing them in a microfluidic channel of similar transverse size. The mechanical properties could be determined with a success rate of 89 % with the inverse analysis process. The results are shown to be repeatable, with a good accuracy, even if some dispersion is observed on the measurement points. This could be due to a small inter-capsule variability for given fabrication parameters.

The profile comparison in Fig. 3 shows a good overlap between the measured and simulated cross-sections for capsules with a concentration of 20 % and higher. This shows that the capsule membrane can be well modeled as a thin hyperelastic sheet, and thus that the cross-linking of the protein present at the interface produces a membrane with elastic properties. We have found that the mechanical resistance of the membrane increases both with HSA concentration and with capsule size. This confirms the recent measurements of de Loubens et al. [19], obtained in elongational flow on large capsules produced with 625 rpm stirring speed.

To further analyze the reason why the resistance is both a function of the HSA concentration and of the capsule size, one has to consider the amount of HSA molecules available to be cross-linked at the interface. In each emulsion droplet of radius a , there are $4\pi a^3[\text{HSA}]/3$ molecules of HSA, $[\text{HSA}]$ being the initial concentration in HSA molecules per unit volume. Due to their amphiphilic character, proteins like HSA tend to adsorb to surfaces and interfaces. Consequently, the maximum surface concentration $[\text{HSA}]_s$ in HSA molecules is $[\text{HSA}]_s = a[\text{HSA}]/3$. The maximum surface concentration in HSA molecules thus increases both with the capsule size and with the initial bulk HSA concentration, as it is proportional to the

product of both parameters $a \times [\text{HSA}]$. For low protein concentrations and/or high stirring speeds, the whole surface area of the emulsion may not be entirely covered by HSA molecules (too low $[\text{HSA}]_s$), whereas for high initial protein concentrations and/or low stirring speeds, all the HSA molecules may not be in contact with the interface (too high $[\text{HSA}]_s$). In the intermediate case, HSA molecules are more or less spread at the interface. The rate of protein adsorption at interfaces depends on the protein type. Contrary to ovalbumin, HSA is known to be a “soft” globular protein, rapidly adsorbing at interfaces and which tertiary structure can easily modify to facilitate the adsorption [29, 31]. For a high protein concentration, the whole interfacial area of the emulsion can be rapidly covered with protein without unfolding. The lowering of protein concentration below a threshold value leads to unfolding of the protein, exposing previously buried groups [30]. When the concentration is further lowered, the unfolding can provoke protein denaturation and precipitation [29].

The shear elastic modulus of the capsule membrane obviously depends on the amount of intermolecular cross-links, which in turns, depends on the number (and conformation) of the HSA molecules available at the interface. The latter is indeed the limiting factors in the chemical reaction, since the cross-linking agent is in excess. The fact that G_s increases both with size and with HSA concentration is thus consistent. Moreover, if we plot the shear modulus results in terms of the product of the two parameters $a \times [\text{HSA}]$ (Fig. 8), we find that all the $\overline{G_s}$ values roughly collapse onto a single curve, whereas they were on distinct $[\text{HSA}]$ -dependent curves, when plotted as a function of a alone (Fig. 5). For the concentration $[\text{HSA}] = 30\%$, the values of $\overline{G_s}$ are slightly above the correlation curve. We had

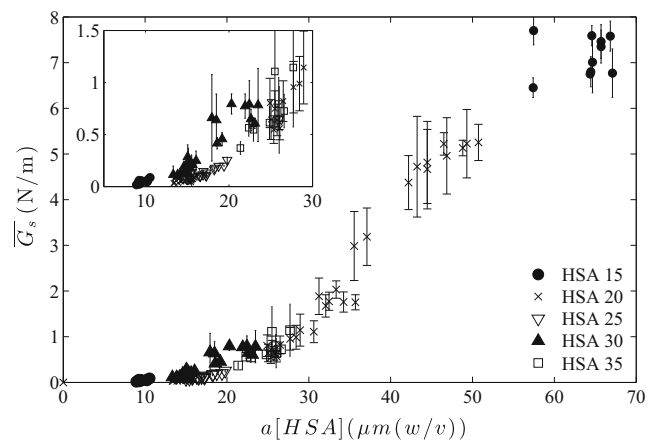


Fig. 8 Evolution of the surface shear modulus $\overline{G_s}$ as a function of $a \times [\text{HSA}]$ for all the capsules. The error bars correspond to $\pm\sigma$. Insert: zoom on small radius

wondered whether it was an indication of a change of protein conformation at the interface from spread and unfolded at low protein concentrations to globular at higher protein concentration [30], but the results obtained for $[HSA] = 35\%$ fit perfectly well with those measured for $[HSA] < 30\%$. This hypothesis therefore does not hold and the phenomenon must be related to possible fabrication or storage variability.

Figure 8 shows that $\overline{G_s}$ tends toward zero for low values of $a \times [HSA]$. The convergence toward a zero asymptotic value for $a \times [HSA] \leq 10$ can be explained by the fact that no continuous insoluble membrane can form around the droplets of the emulsion, when not enough HSA molecules are present to coat the interface and lead to the formation of a membrane. In practice, using the reaction conditions chosen for the study, no capsules could, for instance, be fabricated at 1700 rpm with an HSA concentration lower than 15 %: this proves that a minimum amount of serum albumin is necessary to form a closed membrane upon cross-linking. $[HSA] = 15\%$ thus corresponds to a limit in the fabrication process for 1700 rpm. This explains why it is difficult to draw definite conclusion regarding the behavior of $\overline{G_s}$ for the HSA15 capsules. The fit between the numerical and experimental deformed capsule profiles shows a slight difference at the back of the experimental capsule contrary to the other cases shown in Fig. 3. The rear of the capsule is more rounded than that of the numerical one, which could be linked to a thickening of the membrane and thus to a non-negligible bending energy for this concentration. The absence of bending energy in the numerical simulations would explain why the experimental-numerical comparison is then less good. The reason to this thickening is not quite clear at present, but it could be due to an accumulation of loose cross-linked HSA network convected by flow toward the rear of the capsule. It could also be due to protein precipitation provoked by the intense unfolding at this low concentration [29]. Two phenomena would then superimpose, protein cross-linking leading to an elastic deformable membrane when no precipitation occurs, and protein precipitation leading to a rigid and less deformable membrane.

No conclusion on the asymptotic behavior of $\overline{G_s}$ for high values of $a \times [HSA]$ can be drawn from the present results. A quasi-linear increase of $\overline{G_s}$ is observed in the range $20 \leq a \times [HSA] \leq 60$, but would the mechanical resistance of the capsules converge toward an asymptotic value for higher values of the product? Increasing the concentration in HSA does not enable to investigate the high $a \times [HSA]$ domain: Fig. 8 indeed shows that the HSA30 and HSA35 capsules have $a \times [HSA]$ values centered onto 20. This parameter domain could possibly be investigated by increasing the capsule size, but low HSA concentration would thus be required. It is thus not for

granted that higher values of the $a \times [HSA]$ product would be reached.

Conclusion

We have used a chemical reaction at an interface between an hydrophilic and an hydrophobic medium in order to elaborate a closed membrane forming a spherical capsule. Cross-linking human serum albumin by means of terephthaloyl chloride enables the fabrication of capsules that have potential biomedical applications. Mechanical properties of the membrane have been determined by inverse analysis: flowing capsules in a confined channel exerts a distributed force and modifies the initial spherical shape. Comparing the morphology of hydrodynamically deformed capsules to the one obtained by numerical simulation using a boundary integral method has allowed us to determine the surface shear modulus G_s of the membrane for almost all the capsules (success rate of 89 %). We have measured shear moduli that vary over two orders of magnitude, which shows that the experimental setup can accommodate characterizing capsules with a large range of G_s by using various channel sizes and flow velocities.

The chemical process of membrane fabrication has led us to control both the stirring speed and the HSA concentration, which were thought to be related to the mean capsule size and cross-linking degree, respectively. However, capsules prepared under the same conditions (HSA concentration, stirring speed, cross-linking time) have different values of surface resistance depending on their size. This result is important, because capsules produced in batch using emulsification processes have a significantly large distribution of sizes. The results of the study (Fig. 8) show that the surface shear modulus G_s can increase by a factor 450, when the capsule radius a increases by a factor 6. Actually, G_s increases with the product $a \times [HSA]$, which corresponds to the maximum surface concentration if all the HSA molecules initially present in the volume of the initial sphere were cross-linked at the interface to form the membrane. At low values of $a \times [HSA]$, G_s reaches a zero asymptotic value. When the product is increased, the mechanical resistance varies quasi-linearly with $a \times [HSA]$. The mechanical behavior of capsules characterized by $a \times [HSA] \geq 70$ cannot be investigated by increasing the initial protein concentration, as only small capsules can then be produced.

Our results have put in evidence a striking phenomenon: the strong variation of the surface shear modulus with the capsule size. Consequently, the only option to obtain microcapsules with similar mechanical resistance is to use fabrication techniques that produce monodisperse capsules [6, 28] or to sort capsules by size. Microfluidics has brought new devices and techniques to create batches of

quasi-monodisperse capsules (e.g., Shields et al. [26] for cell sorting). Resorting to them will be a necessity in all the applications where a uniformity in capsule size and mechanical properties is required to ensure a good control of the protection or release of the encapsulated substance.

Acknowledgments Part of the measurements on the small capsules were performed by Océane Ly and Van Tuan Dang.

Compliance with ethical standards

Funding The research study was funded by the French Agence Nationale de la Recherche (CAPSHYDR grant ANR-11-BS09-013 and the Labex MS2T ANR-11-IDEX-0004-02, Labex MEC ANR-10-LABX-0092, A*MIDEX project ANR-11-IDEX-0001-02 within the program “Investment for the Future”) and by the French Ministry of Research (Pilcam2 grant).

Conflict of interest The authors declare that they have no conflict of interest.

References

- Andry MC, Edwards-Lévy F, Lévy MC (1996) Free amino group content of serum albumin microcapsules. III. A study at low pH values. *Int J Pharm* 128:197–202
- Banquet S, Gomez E, Nicol L, Edwards-Lévy F, Henry JP, Cao R, Schapman D, Dautreux B, Lallemand F et al (2011) Arteriogenic therapy by intramyocardial sustained delivery of a novel growth factor combination prevents chronic heart failure. *Circulation* 124:1059–1069
- Barthès-Biesel D, Diaz A, Dhenin E (2002) Effect of constitutive laws for two dimensional membranes on flow-induced capsule deformation. *J Fluid Mech* 460:211–222
- Carin M, Barthès-Biesel D, Edwards-Lévy F, Postel C, Andrei DC (2003) Compression of biocompatible liquid-filled HSA-alginate capsules: determination of the membrane mechanical properties. *Biotechnol Bioeng* 82:207–212
- Chu T, Salsac AV, Leclerc E, Barthès-Biesel D, Wurtz H, Edwards-Lévy F (2011) Comparison between measurements of elasticity and free amino group content of ovalbumin microcapsule membranes: discrimination of the cross-linking degree. *J Colloid Interface Sci* 355(1):81–88
- Chu T, Salsac AV, Barthès-Biesel D, Griscom L, Edwards-Lévy F, Leclerc E (2013) Fabrication and in-situ characterization of microcapsules in a microfluidic system. *Microfluid Nanofluid* 14(1):309–317
- Diaz A, Barthès-Biesel D (2002) Entrance of a bioartificial capsule in a pore. *CMES* 3(3):321–337
- Dimova R, Aranda S, Bezlyepkina N, Nikolov V, Riske K, Lipowsky R (2006) A practical guide to giant vesicles. Probing the membrane nano regime via optical microscopy. *J Phys: Condens Matter* 18:S1151–S1176
- Dubreuil F, Elsner N, Fery A (2003) Elastic properties of polyelectrolyte capsules studied by atomic-force microscopy and rcm. *Eur Phys J E* 12:215–221
- Edwards-Lévy F (2011) Microparticulate drug delivery systems based on serum albumin. In: Serum albumin: structure, functions, and health impact. Nova Science Publishers, New York
- Glycerine Producer’s Association (1963) Physical properties of glycerine and its solutions. New York
- Granicka L (2014) Nanoencapsulation of cells within multi-layer shells for biomedical applications. *J Nanosci Nanotechnol* 14:705–716
- Hochmuth R (2000) Micropipette aspiration of living cells (review). *J Biomechanics* 33:15–22
- Hu XQ, Sévénie B, Salsac AV, Leclerc E, Barthès-Biesel D (2013) Characterization of membrane properties of capsules flowing in a square-section microfluidic channel: effects of the membrane constitutive law. *Phys Rev E* 87:063008
- Kolesnikova T, Skirtach A, Möhwald H (2013) Red blood cells and polyelectrolyte multilayer capsules: natural carriers versus polymer-based drug delivery vehicles. *Expert Opin Drug Deliv* 10:47–58
- Lam P, Gambari R (2014) Advanced progress of microencapsulation technologies: in vivo and in vitro models for studying oral and transdermal drug deliveries. *J Control Release* 178:25–45
- Lefebvre Y, Barthès-Biesel D (2007) Motion of a capsule in a cylindrical tube: effect of membrane pre-stress. *J Fluid Mech* 589:157–181
- Lefebvre Y, Leclerc E, Barthès-Biesel D, Walter J, Edwards-Lévy F (2008) Flow of artificial microcapsules in microfluidic channels: a method for determining the elastic properties of the membrane. *Phys Fluids* 20:1–10
- de Loubens C, Deschamps J, Georgelin M, Charrier A, Edwards-Lévy F, Leonetti M (2014) Mechanical characterization of cross-linked serum albumin microcapsules. *Soft Matter* 10:4561–4568
- de Loubens C, Deschamps J, Boedec G, Leonetti M (2015) Stretching of capsules in an elongation flow, a route to constitutive law. *J Fluid Mech* 767:1469–7645
- Lucas N, Legrand R, Breton J, Déchelotte P, Edwards-Lévy F, Fetissov S (2015) Chronic delivery of α -melanocyte-stimulating hormone in rat hypothalamus using albumin-alginate microparticles: effects on food intake and body weight. *Neuroscience* 290:445–453
- Lévy MC, Lefebvre S, Andry MC, Manfait M (1995) Fourier transform infrared spectroscopic studies of cross-linked human serum albumin microcapsules. 3. Influence of terephthaloyl chloride concentration on spectra and correlation with microcapsule morphology and size. *J Pharm Sci* 84(2):161–165
- Orive G, Hernández RM, Gascón AR, Calafiore R, Chang TMS, de Vos P, Hortelano G, Hunkeler D, Lacić L, Pedraz JL (2004) History, challenges and perspectives of cell microencapsulation. *Trends Biotechnol* 22:87–92
- Rachik M, Barthès-Biesel D, Carin M, Edwards-Lévy F (2006) Identification of the elastic properties of an artificial capsule membrane with the compression test: effect of thickness. *J Colloid Interf Sci* 301:217–226
- Radmacher M (2002) Measuring the elastic properties of living cells by the atomic force microscope. *Methods Cell Biol* 68:67–90
- Shields C, Reyes C, López G (2003) Microfluidic cell sorting: a review of the advances in the separation of cells from debulking to rare cell isolation. *Lab Chip* 15:1230–1249
- Sukhorukov G, Möhwald H (2007) Multifunctional cargo systems for biotechnology. *Trends Biotechnol* 25:93–98
- Thorsen T, Roberts RW, Arnold FH, Quake SR (2001) Dynamic pattern formation in a vesicle-generating microfluidic device. *Phys Rev Lett* 86:4163–4166
- Tripp B, Magda J, Andrade J (1995) Adsorption of globular proteins at the air/water interface as measured via dynamic surface tension: concentration dependence, mass-transfer considerations, and adsorption kinetics. *J Colloid Interf Sci* 173:16–27
- Wierenga P, Egmond MR, Voragen AGJ, de Jong HHJ (2006) The adsorption and unfolding kinetics determines the folding state of proteins at the air-water interface and thereby the equation of state. *J Colloid Interf Sci* 299:850–857
- Yano Y (2012) Kinetics of protein unfolding at interfaces. *J Phys: Condens Matter* 503101